Compatibility of Poly(vinylidene fluoride) (PVDF)/Polyamide 12 (PA12) Blends

LEE KEUN YOON, BYUNG KYU KIM

Department of Polymer Science and Engineering, Pusan National University, Pusan 609-735, Korea

Received 18 September 1999; accepted 14 February 2000

ABSTRACT: Poly(vinylidene fluoride) (PVDF)/polyamide 12 (PA12) blends showed new peaks in XRD profile with increasing PA12 and the crystallinity of PA12 significantly decreased with the addition of PVDF. PVDF showed three relaxation regions at about −40, 40, and 100°C, respectively, and glass transition temperature (T_g) of PA12 increased in blends (10.8→30.14°C) and α-relaxation of PVDF decreased from 100.26 to 86.46°C. Complex viscosities (η^*) vs. composition curve showed a great positive deviation in PVDF-rich and a small negative deviation in PA12-rich blends. The N—H and C=O stretching band of PA12 shifted slightly toward higher wavelength, and from curve-fitted data the area of hydrogen-bonded C=O stretching bands of PA12 decreased with the addition of PVDF, especially in the 30/70 blend, implying the existence of interactions between the β-hydrogen atom of PVDF and amide carbonyl group of PA12 in the blends. © 2000 John Wiley & Sons, Inc. J Appl Polym Sci 78: 1374–1380, 2000

Key words: poly(vinylidene fluoride) (PVDF); polyamide 12 (PA12); compatibility

INTRODUCTION

In the past several decades, a considerable amount of research has been aimed at gaining a better understanding of the miscibility of polymers.[1,2] Miscibility of different polymers is driven by crossintermolecular interactions. The stronger these interactions are, the greater the tendency to miscibility is, showing inward shifts of glass transition temperatures (T_g) of constitutive polymers in the blends. Conversely, a polymer pair is immiscible when the interactions in the constitutive polymer are much stronger than in the blend, showing two separated T_gs in blend. This situation would prevail in polar polymer blends such as poly(vinylidene fluoride) (PVDF)/polyamide 6 blends as a result of much stronger hydrogen bonding in the constitutive polymers. This effect could explain the immiscibility of these two polymers, which has been observed by a set of techniques such as dynamic mechanical analysis and differential scanning calorimetry.[3,4]

On the other hand, domain size of dispersed phases is controlled by a series of experimental parameters, such as blend composition, relative polymer melt viscosities, and processing conditions, as well as chain structure. Furthermore, all the other conditions being the same, the average particle size increases with increasing interfacial tension.[5,6]

In this experiment, we studied the miscibility of PVDF/polyamide 12 (PA12) blends over the full composition range in terms of crystallographical, dynamic mechanical, morphological, rheological, and thermal properties. Particularly, Fourier transform infrared (FTIR) analysis showed interaction between PVDF and PA12 more precisely.

Correspondence to: B. K. Kim.

Contract grant sponsor: Korea Science and Engineering Foundation.

Journal of Applied Polymer Science, Vol. 78, 1374–1380 (2000)

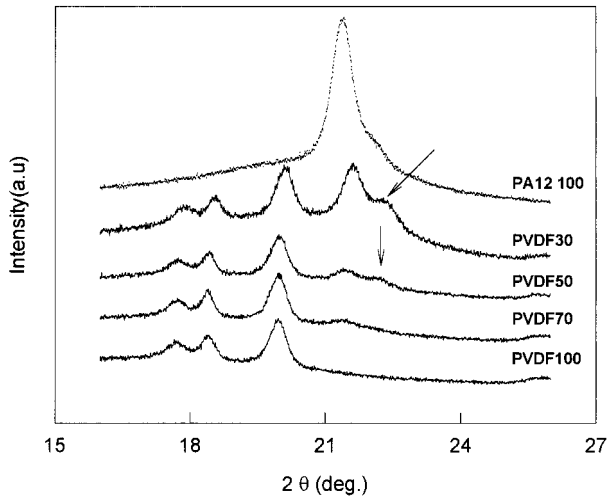

Figure 1 XRD profiles of PVDF, PA12, and PVDF/PA12 blends.

EXPERIMENTAL

PVDF(X7394, ρ = 1.76 g/cm^3) and polyamide 12(X7293, ρ = 1.03 g/cm^3) were purchased from Dycell Hüls and dried at 80°C for 1 day in a convection oven before blending.

Melt blends of 100/0, 70/30, 50/50, 30/70, and 0/100 (PVDF/PA12) (vol/vol%) were prepared using a Haake twin screw extruder at 220°C, 50 rpm followed by pelletizing and drying at 100°C for 2 days. Samples were compression molded using a hydraulic press at 220°C to prepare specimens for rheological, dynamic mechanical, morphological, and crystallographic tests, and FTIR analysis.

Crystalline structures of the base resin and blends were determined by a wide-angle X-ray diffractometer (XRD) (Rigaku 2013) using CuKα at 30 kV, 15 mA, with a scan speed of 2.2°/min.[7] Compression-molded samples were mounted along the through direction. Rheological properties were measured using a Rheometrics Dynamic Analyzer (RDA) II with a parallel plate fixture (gap = 2.0 mm) at 220°C. The strain level was kept at 10%.

Dynamic mechanical properties were measured using a dynamic mechanical thermal analyzer (DMTA) (Rheometer MK3) at 110 Hz and at a heating rate of 3°C/min from −50 to 180°C. Morphologies were observed using scanning electron microscopy (SEM, JSM6400). SEM micrographs were taken from cryogenically (in liquid nitrogen) fractured surfaces of compression-molded specimens. Surfaces were sputtered with gold before viewing. Crystalline melting temperature (T_m) and crystallization temperature (T_c) were measured by a differential scanning calorimetry (DSC) (Du Pont 910 Thermal Analyzer). Samples (ca. 5 mg) were heated from room temperature to 200°C at 20°C/min, held for 5 min and cooled to room temperature, with nitrogen purging, recording the exotherms. Samples were reheated to 200°C at the same heating rate, while recording the endotherms. The characteristic absorption peaks in FTIR spectrophotometry were used to investigate the interactions between PVDF and PA12.

RESULTS AND DISCUSSION

X-ray Diffractograms

Depending on the method of sample preparation PVDF shows polymorphism where five crystalline

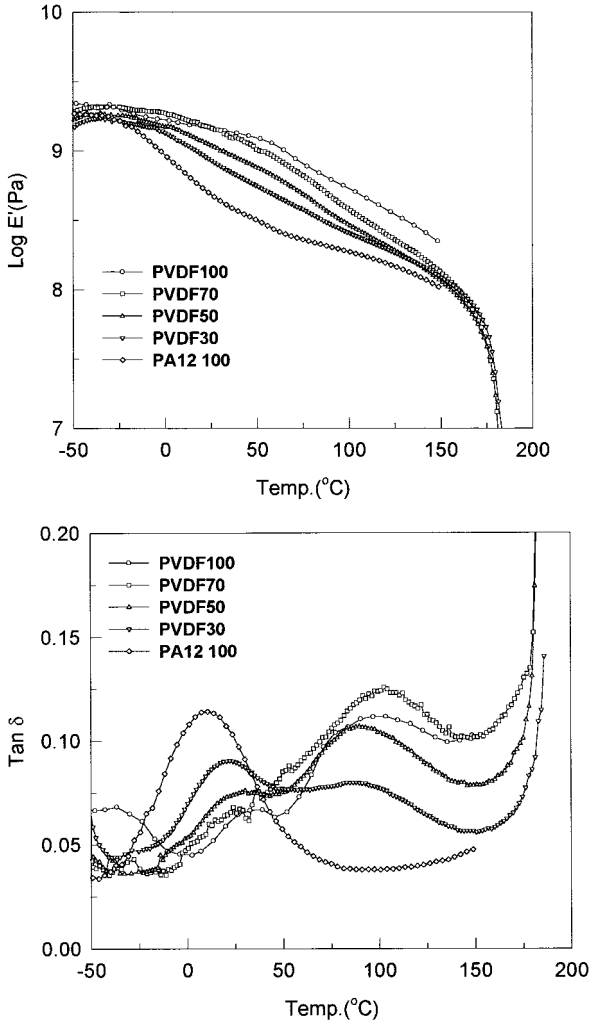

Figure 2 Dynamic mechanical properties of PVDF, PA12, and PVDF/PA12 blends; (a) E', and (b) tan δ.

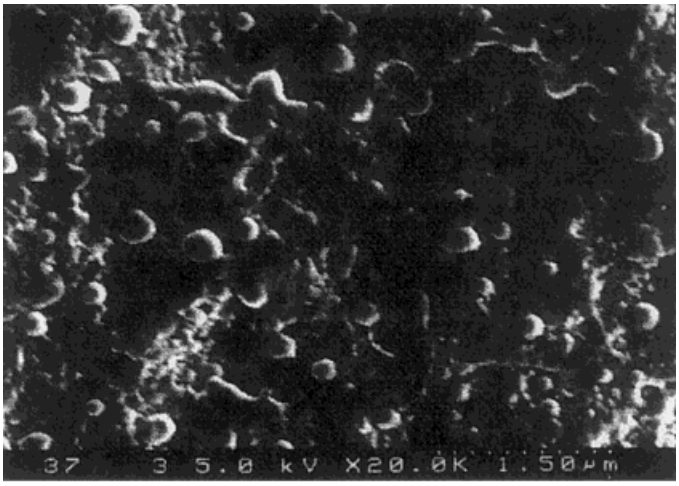

(a) PVDF/PA 12 = 70/30

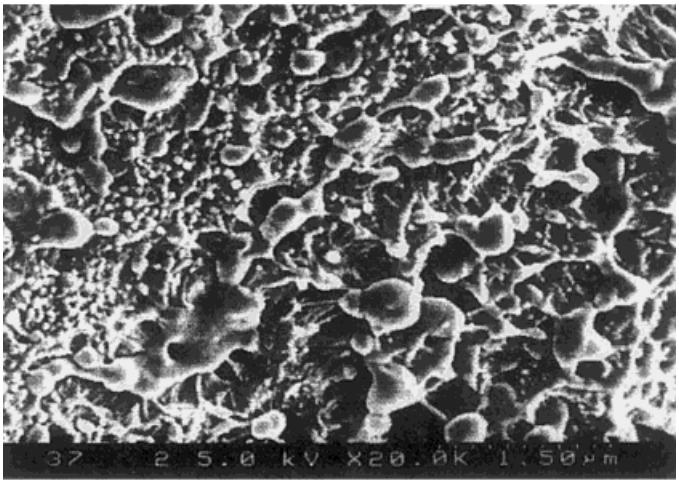

(b) PVDF/PA 12 = 50/50

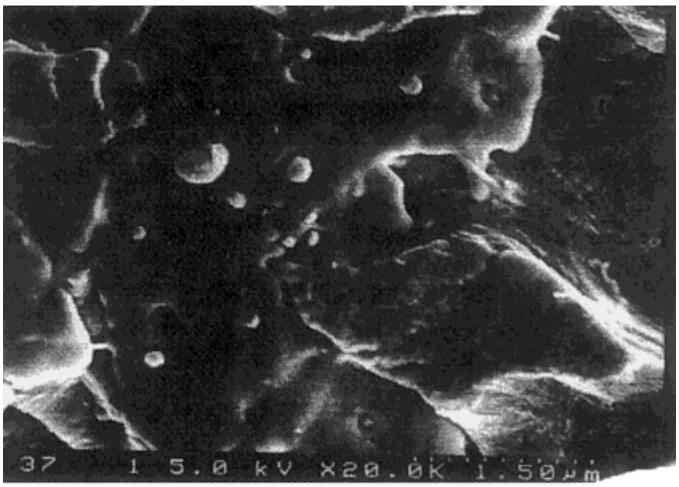

(c) PVDF/PA 12 = 30/70

Figure 3 SEMs of PVDF/PA12 blends.

phases, designated as α, β, γ, δ, and ϵ[8,9] are observed. If the polymer is melt crystallized under atmospheric pressure, an α-phase, in which polymer backbone is in a *trans-gauche-gauche* configuration, is produced.[10]

Figure 1 shows X-ray diffractograms of the base resins and PVDF/PA12 blends. The crystalline structure of PVDF is pseudo-orthorhombic (α-phase) with $2\theta = 17.68(100)$, 18.41(020), 19.96(110), 25.69(120), 26.58(021), and 27.81(111), which are well agreed with those reported by Gregorio and Cestari.[11] The main peak ($2\theta = 19.95$) of PVDF does not change with blend composition except for the 30/70 blend (19.95°→20.08°), whereas that of PA12 slightly shifts toward higher degree (21.42°→21.63°) accompanied by decreased peak intensity, implying that the crystalline structure of PA12 becomes less perfect in the blends.

On the other hand, a small peak, which was not observed in both of the base resins, is shown at $2\theta = 22.36$ and 22.38 in 50/50 and 30/70 blends, indicative of certain interactions between PVDF and PA12.

Dynamic Mechanical Properties

Figure 2 shows dynamic mechanical properties of the base resins and PVDF/PA12 blends. Lovinger and Wang[12] have reported that PVDF exhibits two distinct relaxations, namely the α-relaxation at around 80°C related to chain vibrations in the crystalline phase, and the β-relaxation related to glass transition at about −30°C. Sometimes, a much smaller relaxation (γ) can be detected at the still lower temperature of −60°C which, however, in most instances merges into the β-relaxation. A fourth weak relaxation (β') is located at 40°C. Our results show three relaxation peaks at −40(β), 40(β'), and 100°C(α), respectively [Fig. 2(b)]. PVDF shows α-relaxation at about 55°C, and shifts toward lower temperature with increasing PA12 content [Fig. 2(a)]. The dispersion of PVDF at glass transition (−40°C) disappears with the 70/30 blend [Fig. 2(b)], and the β' region of PVDF at 40°C becomes a shoulder and eventually disappears with the addition and increase of PA12. T_g (10.8°C) of PA12 increases by about 20°C (30.1°C at 50/50 blend). Transition of PVDF at 100°C decreases by about 15°C (86.5°C at 30/70 blend). It seems that the transition of PVDF at about 100°C is most sensitive to the blending with PA12.

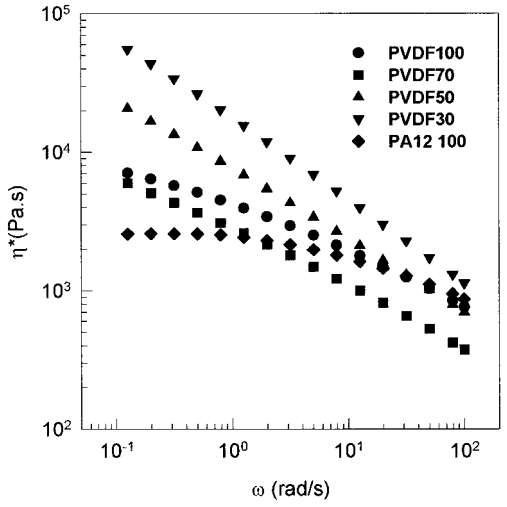

Figure 4 Complex viscosity (η^*) of PVDF, PA12, and PVDF/PA12 blends as a function of frequency (220°C).

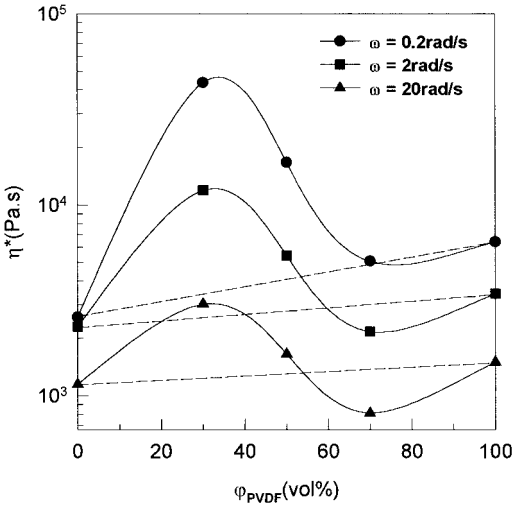

Figure 5 Complex viscosity (η^*) of PVDF, PA12, PVDF/PA12 blends as a function of PVDF content at various frequencies (220°C).

Morphology

Figure 3 shows SEM micrographs of PVDF/PA12 blends where PA12 forms dispersed domains in the 70/30 blend [Fig. 3(a)], and PVDF domains in 50/50 and 30/70 blends. However, the number and fractional area of PVDF domains in the 30/70 blend is much smaller than those of PA12 in 70/30 blend. It seems that the solubility of PVDF in PA12 is greater than that of PA12 in PVDF, due to the greater intermolecular interactions evidenced from the XRD profiles (Fig. 1). Similar

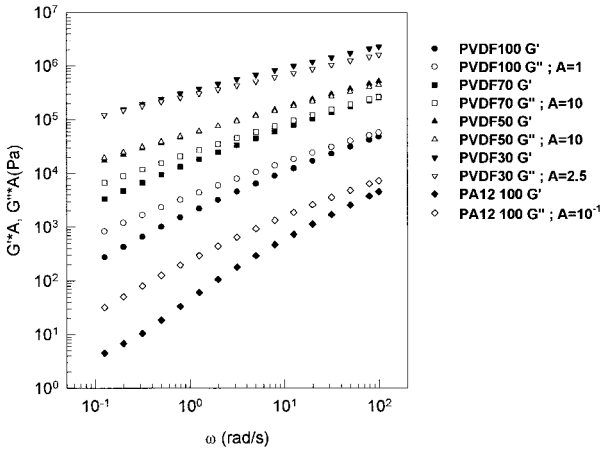

Figure 6 G' and G'' of PVDF, PA12, and PVDF/PA12 blends as a function of frequency (220°C).

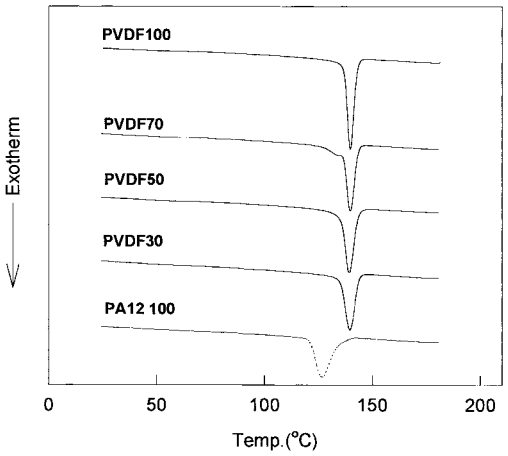

Figure 8 Crystallization exotherm of PVDF, PA12, and PVDF/PA12 blends.

results were also reported by Liu et al.,[13] where the average size of the dispersed phase was of 0.2–1.0 μm with PVDF dispersion, and 0.5–1.0 μm in the reverse situation in PA 6/PVDF blends. However, our results on PVDF/PA12 showed smaller domain size especially in the 50/50 blend, implying that PA12 is more compatible with PVDF.

Rheological Properties

Figure 4 shows melt viscosity (η^*) of the base resins and PVDF/PA12 blends as a function of oscillation frequency. The viscosity function of PVDF is a straight line in log-log plot, resembling the behavior of an elastomer. On the other hand, the viscosity function of PA12 is that of a typical thermoplastic with a Newtonian plateau at low frequencies. At low frequency, η^* of PVDF is several times greater than that of PA12. Viscosity vs. composition plot at three different frequencies is also given in Figure 5. A large positive deviation

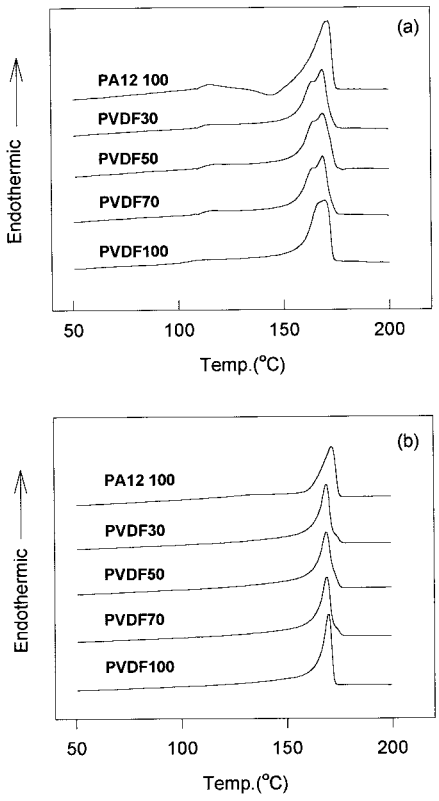

Figure 7 Melting endotherm of PVDF, PA12, and PVDF/PA12 blends; (a) first scan, and (b) second scan.

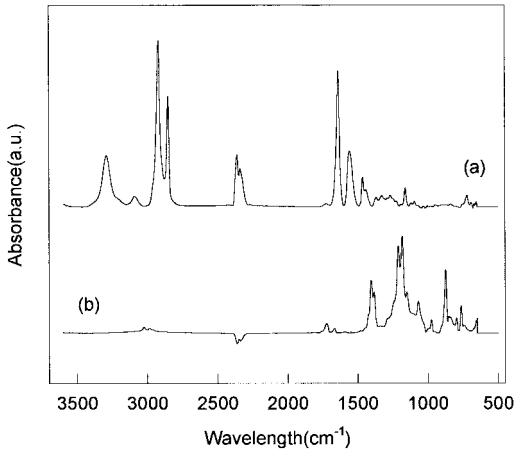

Figure 9 FTIR spectra of PA12 (a) and PVDF (b).

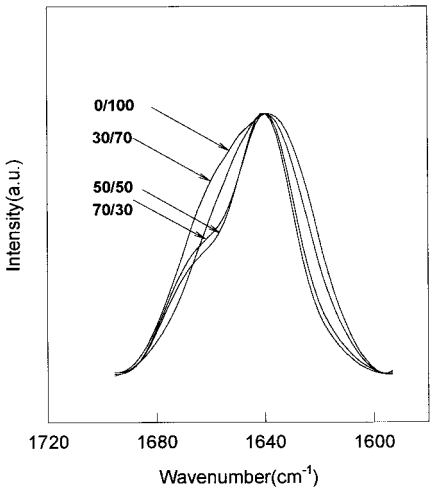

Figure 10 The C=O stretching band of PA12 in PVDF/PA12 blends.

in PA12-rich, and a small negative deviation in PVDF-rich blends are observed. It has been reported that PVDF-rich phases do not well mix with other polymers, and this should be a cause of viscosity rise of the blend. Positive and negative deviations sometimes occur when there is a phase inversion at a certain blend composition.[14] Based upon this, the phase inversion should occur at around 70/30. However, our results do not confirm this.

Figure 6 shows storage (G') and loss (G'') moduli of the blends as a function of frequency. A crossover point between G' and G'' was not obtained with the base resins. However, crossover points appear in the blends and they shift toward low frequency as the content of PA12 increases, indicative of increasing intermolecular entanglements between PVDF and PA12.[15]

Thermal Properties

Figures 7 and 8 show DSC thermograms for PVDF, PA12, and PVDF/PA12 blends. Crystalline melting temperatures (T_m) of PVDF and PA12 are 169.4 and 171.6°C, respectively. T_m of PA12 as well PVDF decreases in the blends, indicating that there are some interactions in amorphous domains. The relatively broad melting endotherm of PVDF is due to the crystal distribution by quenching from melt [Fig. 7(a)]. PA12 shows broad heating crystallization over 110–135°C. However, second scan [Fig. 7(b)] and cooling curves (Fig. 8) show a single peak. It is noted that the crystallization temperature upon cooling (T_c) of the blends is the same as with PVDF, which is higher than that of PA12 by about 15°C.

It is noted that PVDF and blends show shoulders on the low temperature side of the main melting peak [Fig. 7(a)]. This is probably due to the annealing effect of PVDF during drying of the base resins at 100°C, which was also reported by others.[15] This is similar to α-relaxation of DMTA data. However, it is not observed during the second scan [Fig. 7(b)].

FTIR Analysis

Figure 9 shows FTIR spectra of PVDF and PA12. PVDF shows the presence of the α-phase at 1384, 976, 874, and 852 cm^{-1}, which agrees well with Benedetti et al.[16] Figure 10 shows the C=O stretching bands of PA12 in PVDF/PA12 blends and curve-fitting results are listed in Table I. The area of hydrogen-bonded C=O stretching bands of PA12 decreases significantly with the 30/70 blend (0.80→0.62). This implies that the β-hydrogen atom of PVDF interacts with amide carbonyl group of PA12. It has been reported that the spe-

Table I Curve-Fitting Results of the C═O Stretching Bands in PVDF/PA 12 Blends

	Hydrogen-bonded			Free					
	$\nu(cm^{-1})$	$W_{1/2}$[a]	A_h[b]	$\nu(cm^{-1})$	$W_{1/2}$	A_f[c]	A_T[d]	A_h/A_T	A_f/A_T
0/100	1638	34	36.7	1663	28	9.3	46.0	0.80	0.20
30/70	1635	32	32.6	1660	30	20.0	52.6	0.62	0.38
50/50	1640	30	32.7	1668	21	8.7	41.4	0.79	0.21
70/30	1640	28	31.0	1668	21	8.2	39.2	0.79	0.21

[a] Width at half-height of peak.
[b] Area of hydrogen-bonded C═O bands of PA 12.
[c] Area of free C═O bands of PA 12.
[d] $A_T = A_h + A_f$.

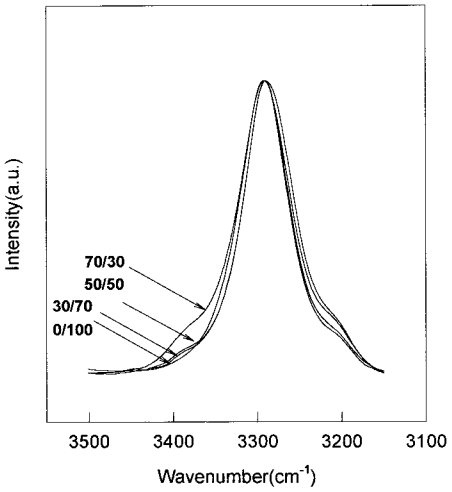

Figure 11 The N—H stretching band of PA12 in PA12 and PVDF/PA12 blends.

cific interactions between PVDF and PMMA would imply the involvement of carbonyl groups in PMMA.[17] Therefore, it seems reasonable that the specific interactions prevailing in PVDF/PA12 blends are hydrogen bonds between the carbonyl of the PA12 amide groups and β-hydrogen atoms of PVDF. Figure 11 shows the N—H stretching bands of PA12 in PVDF/PA12 blends. The area and position of the peak do not change with increasing PVDF content, except for the 30/70 blends. As a result, PA12-rich blends are more compatible than PVDF-rich blends.

CONCLUSIONS

It may be concluded that PVDF/PA12 blends are partially miscible due to the hydrogen bondings between the carbonyl of PA12 amide group and β-hydrogen atoms of PVDF, as evidenced from the FTIR analysis. Domain size of PVDF in PA12-rich blends was smaller than that of PA12 in PVDF-rich blends. This should be related to a greater positive deviation in melt viscosity in PVDF-rich blends. The partial miscibility led to a decrease in T_m of PA12 and as well as PVDF in the blends.

Financial support by Korea Science and Engineering Foundation through Hyperstructured Organic Materials Research Center is gratefully acknowledged.

REFERENCES

1. Paul, D. R.; Newman, S. Polymer Blends; Academic Press: New York, 1978.
2. Choi, C. H.; Kim, B. K. Polym Eng Sci 1996, 36, 1495.
3. Liu, Z. H.; Maréchal, Ph.; Jérome, R. Polymer 1997, 38, 5149.
4. Liu, Z. H.; Maréchal, Ph.; Jérome, R. Polymer 1997, 38, 4925.
5. Wu, W. Polym Eng Sci 1987, 27, 335.
6. Serpe, G.; Jarrin, J.; Dawans, F. Polym Eng Sci 1990, 30, 553.
7. Choi, C. H.; Yoon, L. K.; Kim, B. K. J Appl Polym Sci 1996, 60, 779.
8. Lovinger, A. J. Science 1983, 220, 1115.
9. Chen, L. T.; Franck, C. W. Ferroelectrics 1984, 57, 51.
10. Takahashi, Y.; Tadokoro, H. Macromolecules 1980, 12, 1317.
11. Gregorio, R., Jr.; Cestari, M. J Polym Sci Part B Polym Phys 1994, 32, 859.
12. Lovinger, A. J.; Wang, T. T. Polymer 1979, 20, 725.
13. Liu, Z. H.; Maréchal, Ph.; Jérome, R. Polymer 1998, 39, 1779.
14. Han, C. D. Multiphase Flow in Polymer Processing; Academic Press: London, 1981, p. 90.
15. Bouilloux, A.; Ernst, B.; Lobbrecht, A.; Muller, R. Polymer 1997, 38, 775.
16. Benedetti, E.; Catanorchi, S.; D'Alessio, A.; Moggi, G.; Vergamini, P.; Pracella, M.; Ciardelli, F. Polym Int 1996, 41, 35.
17. Bernstein, R. E.; Wahrmund, D. C.; Barlow, J. W.; Paul, D. R. Polym Eng Sci 1978, 18, 1220.